GENESIS OF DONGPING GOLD-TELLURIDE DEPOSIT BASED ON GEOCHEMICAL CHARACTERISTICS OF FLUIDS, ^{40}Ar/^{39}Ar DATING, STABLE AND RADIOGENIC ISOTOPES (NORTH CHINA)

Mamady Cisse[1*], Xinbiao Lü[2], Munir Mohammed Abdalla Adam[2], Ladislav A. Palinkas[3], Algeo J. Thomas[4,5]

[1]*Institut Supérieur des Mines et Géologie de Boké, BP: 84, Conakry, Republic of Guinea*
[2]*Faculty of Earth Resources, China University of Geosciences, Wuhan, Hubei Province 430074, China*
[3]*Faculty of Sciences, Geology Department, University of Zagreb, Horvatovac 95, 10 000 Zagreb, Croatia*
[4]*State Key Laboratory of Biogeology and Environmental Geology, China University of Geosciences, Wuhan, Hubei Province 430074, China*
[5]*Department of Geology, University of Cincinnati, Cincinnati, OH 45221-0013, U.S.A.*
*mcisseismgb@yahoo.fr

A b s t r a c t: The Dongping goldfield is located within the Shuiquangou alkaline complex of the western Yanshan Mountains of Hebei Province, on the northern margin of the North China Craton. It is one of the largest gold deposits in China, with a planned gold production of 2.57 tons annually over a lifespan of 12 years. The Dongping gold deposit is enriched in the elements Au, Te, Ag, Pb, Bi, Sb and As. Most of the gold is present in the telluride minerals calaverite (43% Au, 38% Ag) and petzite (23% Au, 46% Ag). Gold mineralization is hosted mainly by K-feldspar-quartz stockworks, veins and disseminated sulfides. The deposit contains three ore types that are distinguished by their mineral associations: vein quartz gold, telluride gold, and disseminated gold. The paragenesis of the ores exhibits three distinct hydrothermal stages, of which the second one was the main ore-enrichment stage. The ore-related ^{40}Ar/^{39}Ar ages determined on K-feldspar samples indicate two episodes of gold mineralization, at 154.89 ± 0.70 Ma and 176.93 ± 4.66 Ma. The gold mineralization ages thus postdate the Devonian-age granite intrusion but overlap possible Jurassic-Cretaceous magmatic activity. The homogenization temperatures of the majority of inclusions range from 120 to 240°C and from 240 to 400°C. The inclusions in quartz veins are CO_2-rich and characterized by low salinity (average 6.0–8.8 wt% NaCl eq.). The laser Raman spectrum of the inclusions shows that the fluid compositions are dominantly waterrich but also contain CO_2. The hydrogen isotope compositions (δ^2H) of the fluid inclusions range from -100.3 to -66.5 ‰, and the calculated oxygen isotope compositions (δ^{18}O) for source fluids range from -0.3 to $+6.9$ ‰ "Standard Mean Ocean Water" (SMOW). These values indicate that the ore-forming fluid came from a deep magmatic hydrothermal system, with involvement of meteoric water and possibly water affected by organic matter. The sulphur isotope compositions (δ^{34}S) of pyrite are mainly from -0.3 to -13.6 ‰ Vienna Cañon Diablo Troilite (VCDT), suggesting homogeneity of sulphur in the magmatic source with subsequent fractionation under relatively oxidizing conditions in ore-bearing quartz veins. The relationship of δ^2H$_{H2O}$ to ^{87}Sr/^{86}Sr indicates that the fluid inclusions and host granitoid rocks were influenced by mixing of magmatic and meteoric waters.

Key words: Chongli county; Dongping deposit; ^{40}Ar/^{39}Ar dating; stable and radiogenic isotopes; ore-forming fluids; gold deposit; North China

1. INTRODUCTION

The Dongping gold deposit is part of a larger gold mining district that extends over an area of ~6,200 km^2 in North China and Inner Mongolia. It is situated near the village of Dongping in Chongli County (Zhangjiakou district), in northwestern Hebei Province, China, at latitude 40°50'47" – 40°53'34"N and longitude 115°18'17" – 115°24'08" W (Figure 1). It contains large proven reserves of

gold (Au) ore. The No. 70 ore body, with ~9 million tons at an average grade of 5 g/t, and the No. 1 ore body, with ~3.3 million tons at an average grade of 6 g/t, account respectively for 64% and 28% of the gold reserves at Dongping (Figure 2) (Chen et al., 2006). The Dongping gold deposit has been extensively studied by ore geologists and geochemists (Lu et al., 1993; Song & Zhao, 1996; Mo, 1996;

Zhang, 1996; Lu et al., 1997; Nie, 1998; Mao & Li, 2001; Fan et al., 2001; Mao et al., 2003; Bao et al., 2003; Bao & Zhao, 2006; Cook et al., 2009).

However, the age of mineralization, the nature of the oreforming processes, and the relationship of the deposit to the country rock remain under debate.
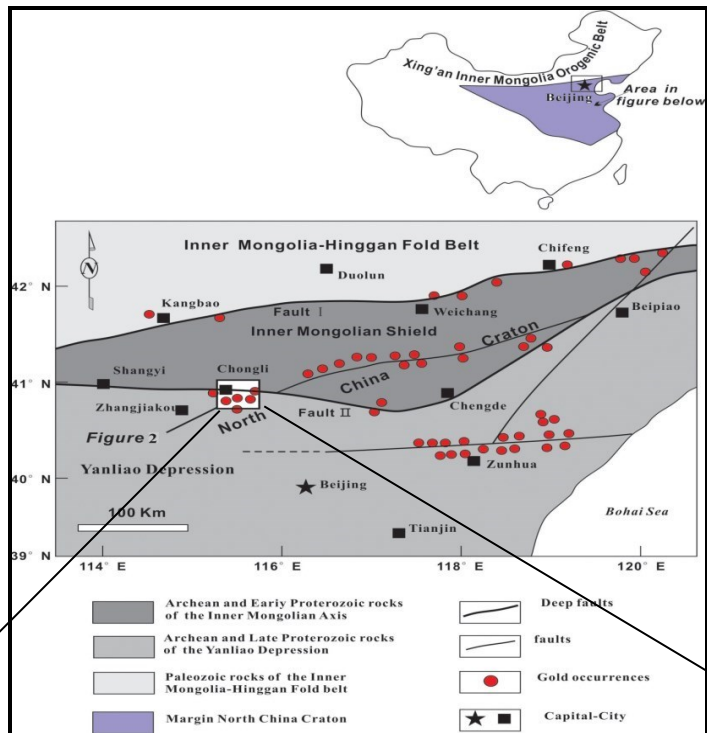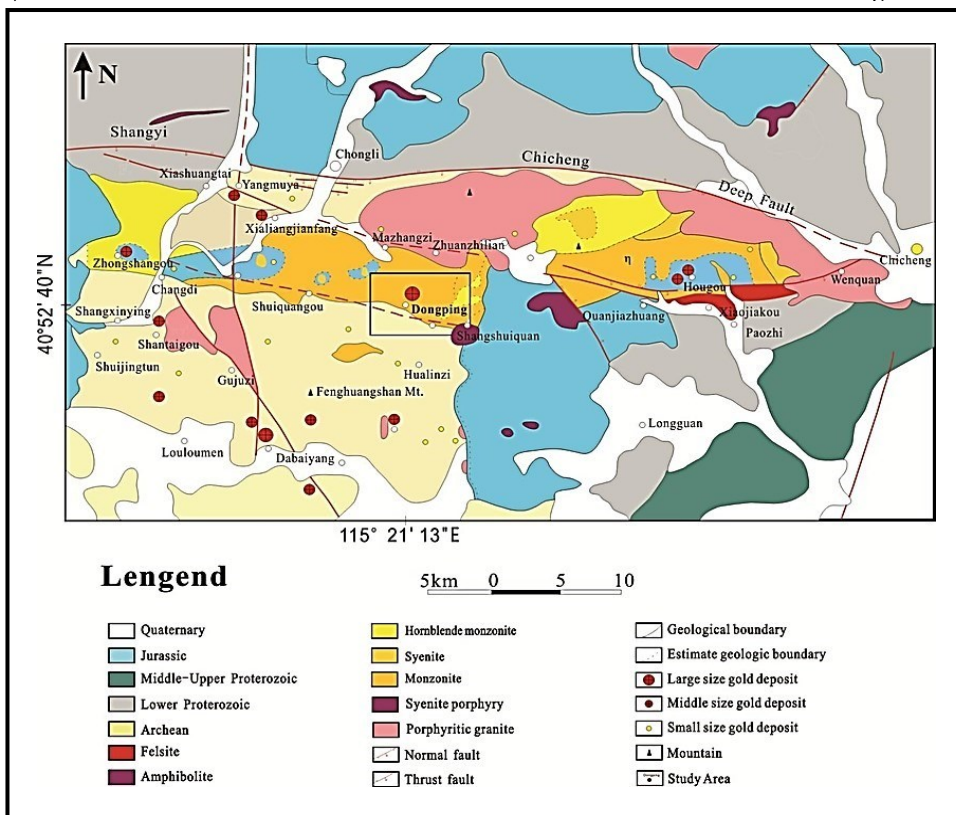
Fig. 1. Simplified geological map of the Dongping goldfield showing the Shangyi Chongli Chicheng deep fault,
Hebei Province, on the northern edge of the North China Craton (NCC)

Fig. 2. The Shuiquangou alkaline complex with gold mineralization along the northern margin of the North China Craton

Application of various dating techniques (UPb, Rb-Sr, Ar-Ar, and K-Ar) has yielded conflicting age results for the Dongping deposit. Recent SHRIMP U-Pb analysis of zircons has documented regional metamorphism of the Archean basement at 2.5 and 1.8 Ga, followed by emplacement of the Shuiquangou syenite-monzonite complex at 390 ± 6 Ma (Luo et al., 2001; Miao et al., 2002; Jiang et al., 2003; Bao et al., 2014). Recent work suggests, however, that ore body formation was coeval with monzogranite emplacement at ~140 Ma, triggered by residual late-magmatic fluid and/or an externally derived hydrothermal fluid generated during a tectonic rifting and underplating event (Miao et al., 2002; Li et al., 2010).

The origin of the Dongping gold deposit has been extensively debated since its discovery. Various theories have been advanced based on inferred differences in the age of gold mineralization and the source of the ore-forming fluids. Some researchers consider the deposit to be of Archean greenstone type (Li, 1999; Wang et al., 1990; Yin, 1994; Yin & Zhai, 1994); orogenic type (Hart et al., 2002; Mao et al., 2003; Miller et al., 1998), whereas others have assigned it to the remobilization type (Bao & Zhao, 2006; Song & Zhao, 1996; Wang et al., 1991); or the alkali porphyry association type (Nie, 1998; Nie et al., 2004; Zhang et al., 2001). The Dongping gold ore has characteristics similar to many intrusion-related deposits (Sillitoe, 2002). Syenite-related gold deposits are usually Te-rich (Te/Au ratio of 0.71) and Cu- and Zn-poor, and they often have an oxidized ore mineral assemblage syngenetic with potassic alteration. The Dongping gold ore has been described variously as an "orogenic mesothermal quartz-vein deposit" *sensu* Goldfarb et al. (2007, 2015), as an "intrusion-related gold system" *sensu* Sillitoe (2002), and an "oxidized intrusion-related gold deposit" (Helt et al., 2014).

The objectives of the present study are to address uncertainties in the origin of the ore-forming fluids, their chemical compositions, and the source of gold-telluride component of the Dongping deposit. We present new data on fluid inclusions, H-O-S isotopes, Sr isotopes, Ar-Ar dating, U-Pb zircon dating, and electron microprobe analysis, and we collate and evaluate these data in relation to data generated in previous studies of the deposit. This analysis permits us to identify the sources of mineralizing fluids, refine the timing of the mineralization event, and reassess the classification of the Dongping gold deposit.

2. GEOLOGIC BACKGROUND

2.1. *Geologic setting of Dongping deposit*

The North China Craton, with an area of 1.5×10^6 km^2, is the largest of the three major Precambrian cratons that comprise China (Wilde et al., 2002). The oldest rocks date to ~3.8 Ga (Wan et al., 2005; Yang et al., 2006), but Nd and Hf isotopes indicate that the main crustal growth event occurred at ~2.7–2.5 Ga (Wu et al., 2006; Yang et al., 2009; Geng et al., 2012; Diwu et al., 2012; Sun et al., 2012; Wang et al., 2013). Seismic profiles suggest that double-polarity Andean-style subduction developed under the Eastern and Western blocks of the craton at ~2.5 Ga, followed by collision with the Columbia supercontinent to the north at ~2.3 Ga (Kusky, 2007). The collision of the Western Block, in which the Dongping gold deposit is located, with the Eastern Block along the ca. 300-km-wide Trans North China Orogen at ~1.85 Ga led to the final amalgamation and stabilization of the North China Craton (Wilde et al., 2002; Kröner et al., 2006; Xia et al., 2006; Zhang-J et al., 2012; Li et al., 2014; Santosh et al., 2010; Santosh et al., 2013).

After amalgamation, the North China Craton remained relatively quiescent with negligible further growth. However, recent studies have revealed later tectonic reactivation of the North China Craton (Gao et al., 2002; Wu et al., 2003; Zheng et al., 2005; Zhang et al., 2012). A multistage thrust fault formed in the Mesoproterozoic and was active in the Neoproterozoic, Paleozoic and Mesozoic (Hu et al., 2003). This long-lived fault system was intruded by a series of ultramafic, alkali and granitic rocks. Large areas on its northern and southern margins were affected by latest Paleozoic to early Mesozoic orogenic events. To the north, closure of the Paleo-Asian Ocean at the end of the Permian and continued convergence during the Triassic and Early Jurassic led to post-collisional thrusting and considerable crust thickening on the northwestern side of the craton (Xiao et al., 2003).

The Shuiquangou alkaline complex is mainly of mid-Paleozoic age (~390 Ma), as indicated by zircon U-Pb dating (Luo et al., 2001; Miao et al., 2003), and was emplaced after the last phase of shearing along the Shangyi-Chongli-Chicheng fault system (Figure 1). Late-stage magmatism led to

emplacement of the Shangshuiquan monzogranite at 142.2±1.3 Ma, which was probably related to an underplating event that took place on the northern margin of the North China Craton at the same time as gold mineralization (Miao et al., 2002). Field relations suggest that the distribution of gold deposits was controlled principally by subsidiary fractures of this fault system (Figure 2). A series of smaller-scale and/or second-order faults are broadly parallel to this fault. The main gold deposits on the northern margin of the North China Craton are distributed along the Chongli Chicheng deep fault, with gold mineralization dominantly along secondary faults and fractures. Other gold deposits are located to the south of this fault, hosted in the Shuiquangou alkaline complex or in Archaean metamorphic rocks.

2.2. *Metallogeny of Dongping deposit*

The metallogeny of the North China Craton is related to its complex tectonic history, which dates to the Archean (Zhai & Santosh, 2011, 2013). The craton has experienced at least five major tectonic cycles: (1) Late Archean crustal growth and stabilization, (2) Paleoproterozoic rifting-subductionaccretion-collision, (3) Late Paleoproterozoic-Neoproterozoic multistage rifting, (4) Paleozoic orogenesis, and (5) Mesozoic extensional tectonics associated with lithospheric thinning and decratonization (Zhai & Santosh, 2011; Zhang-HF et al., 2012). Corresponding to these tectonic cycles are five major metallogenic systems: (1) Archean band iron formation (BIF), (2) Paleoproterozoic copper-lead-zinc and magnesium-boron (Mg-B), (3) Mesoproterozoic rare earth element-iron-lead-zinc (REE-FePbZn), (4) Paleozoic orogenic copper-molybdenum (Cu-Mo), and (5) Mesozoic (Yanshanian) intracontinental gold (Au), silver-lead-zinc (Ag-Pb-Zn), and molybdenum (Mo) systems (Zhai & Santosh, 2013).

Mesozoic gold and molybdenum mineralization in the North China Craton is represented by lode-style Au deposits hosted in Archaean high-grade metamorphic rocks. Dongping gold ore belongs to metallogenic district VIII (Yang et al., 2003; Pirajno, 2013). The Mesozoic mineral systems that occur in the North China Craton are of great economic value, including porphyry, porphyry-skarn, and lode gold deposits, all of which were formed during various phases of the Yanshanian tectono-thermal event (ca. 208–90 Ma). These mineral systems are largely confined to major structures or crustal/lithospheric breaks at the northern

and southern margins of the craton. There are at least three important metallogenic provinces: (1) Jiadong lode Au, (2) Liaoning porphyry, skarns and epithermal belt, and (3) Qinling polymetallic belt, with porphyry, skarns and lode Au-Ag systems (Pirajno, 2013). Mineral systems within the North China Craton can be divided into: (1) those that formed during cratonic amalgamation, (2) those that formed during Paleoproterozoic rifting and igneous activity (e.g., the Xiong'er large igneous province), and (3) those that formed in later times (e.g., in association with the Indosinian or Yanshanian tectonothermal events of Mesozoic age) and which may be hosted in cratonic crust, Paleoproterozoic lithotectonic units, superimposed rift basins, or accreted magmatic arcs (Pirajno, 2013).

Magmatic rocks in the Dongping goldfield region were emplaced in three phases: (1). Proterozoic intrusive rocks, including metamorphic diorite, peridotite and pyroxenite; (2) Hercynian (Variscan) intrusive rocks, mainly the Shuiquangou alkaline complex; and (3) Yanshanian intrusive rocks of Mesozoic age. Gold metallogeny is primarily related to the Variscan Shuiquangou alkaline complex, which is exposed over an area that is ~55 km long (from east to west) and 5 to 8 km wide, parallel to the Shangyi-Chongli-Beipiao deep fault system (Figures 1, 2). This large composite batholith is composed of several syenite-monzonite lithologies, including alkali feldspar syenite, quartz-alkali feldspar syenite, pyroxene-hornblende syenite, hornblendealkali feldspar syenite, pyroxene-hornblende monzonite and hornblende monzonite (Mao et al., 2003). On the basis of the mineral assemblage, petrochemistry and rare earth element geochemistry, Zhang & Mao (1995) divided the Shuiquangou complex into calc-alkaline, weakly alkaline and alkaline series.

The role of the Shuiquangou alkaline complex in gold mineralization along the northern margin of the North China Craton can be traced to the rise of heat and alkaline magma along deep faults, which resulted in melting and alkali metasomatism of hornblende monzonite country rock. These processes contributed to the mobilization of elemental gold in hydrothermal fluids that was subsequently emplaced in the extensive, pre-existing fracture system associated with the Shangyi Chongli-Beipiao deep fault system. The northern margin of the North China Craton is an area with many gold mines, including large-scale deposits at Dongping and Xiaoyingpan, medium-scale deposits at Zhangquanzhuang, Hougou, Huangtuliang, and Shuijingtun, and

small-scale deposits at Zhongshangou, Jinjiazhuang, and elsewhere. In addition to gold ore, this district also yields hematite from the Chuanlinggou formation, lead-zinc silver deposits in metamorphic country rocks, graphite and Anshantype magnetite ore, and coal, talc, magnesite, quartz ore, building stone, and other minerals (Chen et al., 2006; unpublished data).

2.3. *Gold ore and hydrothermal minerals*

The Dongping gold ores are low in sulfides (3 to 5 wt. %), which are mainly pyrite with minor quantities of chalcopyrite, galena, calaverite, altaite, petzite and sphalerite, and lesser amounts of oxides including specularitic hematite and magnetite. Pyrite, which is intimately associated with gold, is most commonly found in the altered wall-rocks which surround the veins. The Dongping mine and nearby gold deposits hosted by the Shuiquangou complex show a number of common features including (i) gold-bearing K-feldsparquartz veins, disseminated sulfide and quartz veins hosted by monzonite and alkaline syenite; (ii) voluminous K-feldspar in early veins; (iii) low quantity of sulfides; (iv) local occurrence of goldbearing tellurides; (v) enrichment of altered host rocks in Au, As, Sb, Bi, Cu, Ag and Pb; and (vi) alteration marked by K-feldspathization, silicification, sulfidization, and carbonization (Nie & Wu, 1995; Zhang & Mao, 1995; Cook et al., 2009).

The alteration zone in the Dongping gold deposit was affected mainly by potassic alteration (quartz, K-feldspar-biotite, ± sericite, ± chlorite) with distal propylitic alteration (chlorite-epidote, ±calcite). The alteration minerals include distinctive reddish K-feldspar (microcline, perthite) and quartz, which are commonly pervasive throughout all ore bodies and the surrounding wall rocks. The chemical composition of the altered area is enriched in Si, K, Au, Te, Cu, Pb and Zn and depleted in Al, Na, Fe, Ca, and Mg. These alteration zones are a product of hydrothermal processes during fluid-rock interactions (Chen et al., 2006).

Typical alteration mineral assemblages at Dongping are shown in Figure 3. The wall rocks surrounding the veins typically contain reddish-colored K-feldspar, forming alteration haloes with a width of a few tens of centimeters; more distally alterations to sericite, chlorite and carbonate are common. The altered wall rocks also carry gold. Among these alteration minerals, secondary K-feldspar is the most abundant and distinctive; moreover, it is usually accompanied by magnetite and quartz. Reddish K-feldspathization and silicification are commonly pervasive throughout the orebodies (Figures 3 b, d).

Fig. 3. Photographs of typical ore-bearing alteration assemblages in the Dongping deposit: (a) altered wall rock with pyrite, intensively silicified; (b) quartz vein cutting K-feldspar-rich altered rock, with gold mineralization; (c) potassic alteration; (d) silicification shown by the white zone; (e) argillization produced by alteration of plagioclase

Three styles of gold mineralization can be differentiated, but there are gradual transitions between them. The first and volumetrically most important type is gold ore within quartz veins containing galena, chalcopyrite and pyrite. The veins are usually 0.5 to 3 m wide and contain fragments of the wall rocks. The second type is gold associated with pyrite in K-feldspar-quartz stockworks and veins. The third type is disseminated gold associated with pyrite and chalcopyrite in altered K-feldspar granitic rocks. In this style of ore, there is a continuous transition between economic ores and the wall rocks. The gold-bearing K-feldspar-quartz and quartz veins are hosted by both monzonite and syenite. Gold in this mine is generally fine-grained and invisible in hand specimen.

We have identified following types of mineralization at Dongping deposit that are distinguished by their modes of occurrence and mineral compositions (i) visible gold in quartz veins; visible gold in K-feldspar-hematite alteration zone and visible gold in K-feldspar monzonite; (ii) weakly altered K-feldspar monzonite with invisible gold in quartz veins, stockworks and disseminated gold contaminated with pyrite, (iii) gold associated with sulfide and oxide minerals (pyrite, galena, chalcopyrite, sphalerite, magnetite and hematite), and (iv) gold-bearing telluride minerals (mainly petzite, calaverite, electrum) (Figure 4). Gold mineralization is less present in carbonate-quartz veins.
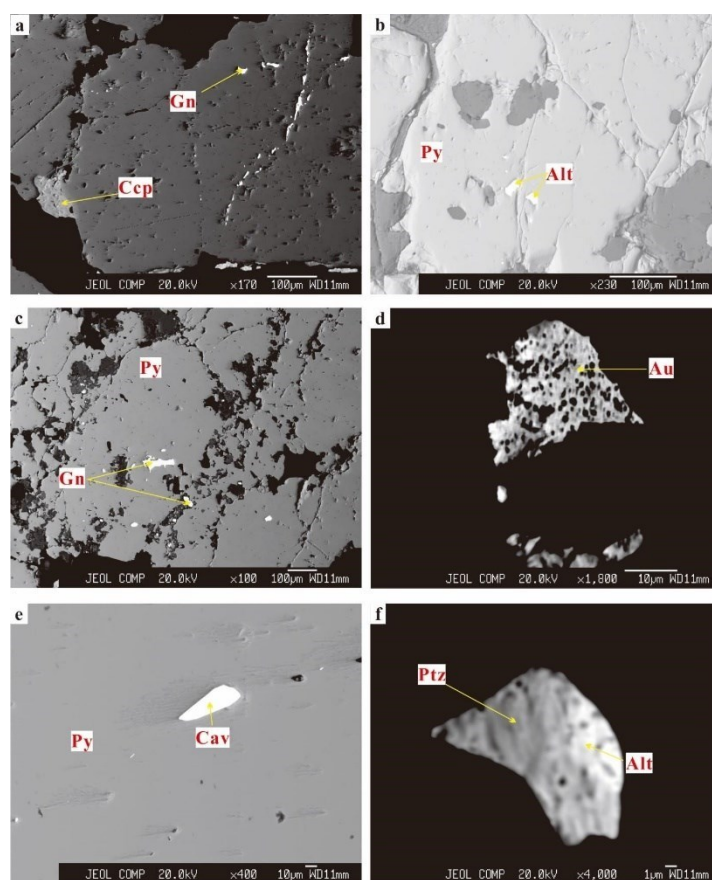
Fig. 4. Backscattered electron images (BSE) of the telluride minerals in the Dongping gold deposit.
Abbreviations: galena (Gn), chalcopyrite (Ccp), pyrite (Py), altaite (Alt), gold (Au), calaverite (Cav) and petzite (Ptz)

3. MATERIALS AND METHODS

3.1. *Electron microprobe analyzer*

Mineral compositions were determined at the State Key Laboratory of Geological Processes and Mineral Resources (GPMR), China University of Geosciences – Wuhan, with a JEOL JXA-8100 Electron Probe Micro Analyzer (EPMA) equipped with four wavelength-dispersive spectrometers (WDS). The following standards were used: arsenide (As), platinum (Pt), gold (Au), selenium (Se), pyrite (S, Fe), chromium (Cr), galena (Pb), bismuth (Bi), cobalt (Co), silver (Ag), nickel (Ni), stibnite (Sb), copper (Cu), tellurium (Te) and sphalerite (Zn) at GPMR (Table 1, Figure 4).

T a b l e 1

Electron probe microanalytical (EMPA) data from whole rock and telluride minerals in Dongping (samples wt.%)

Minerals	Samples DP	As	Pt	Au	Se	S	Cr	Pb	Fe	Bi	Co	Ag	Ni	Sb	Cu	Te	Zn	Total
Pyrite FeS₂	16–6–01	–	–	0.008	–	**52.658**	0.004	0.115	**46.725**	–	0.065	–	0.009	0.009	–	0.022	–	99.615
Altaite PbTe	16–6–02	–	0.042	–	0.004	0.305	0.296	**60.646**	1.735	0.263	–	–	–	0.243	0.016	**37.286**	0.004	100.84
Pyrite FeS₂	**17–7–01**		0.003	0.055	–	**52.924**	–	0.162	**46.501**	0.010	0.072	0.013	0.016	–	0.022	–	–	99.778
	17–10–01	0.016	–	0.016	–	**52.701**	0.003	0.172	46.666	0.012	0.096	0.024	0.001	–	0.016	–	0.009	99.732
Galena PbS	17–10–02	–	–	–	0.020	**13.261**	0.069	**86.290**	1.085	0.332	–	–	–	–	–	0.149	–	101.21
Petzite Ag₃AuTe₂	16–6–03	–	–	**23.537**	0.024	0.293	0.070	1.047	1.850	0.118	–	**38.288**	0.016	0.078	–	**31.983**	0.007	97.311
	16–6–04	–	–	**19.828**	0.006	0.256	0.081	–	1.697	0.171	–	**45.994**	0.045	0.118	0.001	**35.345**	0.005	103.55
Altaite PbTe	16–6–05	–	–	–	–	0.228	0.181	**56.615**	2.425	0.223	–	0.162	0.017	0.219	–	**34.691**	–	94.76
	16–6–06	–	–	–	0.005	1.917	0.261	**58.356**	3.636	0.196	0.019	0.091	–	0.192	–	**34.830**	–	99.503
Native gold	**17–7–04**	0.005	–	**91.044**	0.003	0.086	1.759	–	0.694	0.505	0.022	**3.052**	0.015	–	–	–	0.018	97.203
Galena PbS	17–10–03	0.015	–	–	–	**13.095**	0.388	**85.030**	2.019	0.397	0.020	0.006	0.005	0.029	0.017	0.193	0.004	101.22
	17–10–04	0.007	–	–	–	**13.341**	0.207	**85.604**	1.347	0.320	0.009	0.012	0.016	0.033	–	0.162	–	101.06
Chalcopyrite CuFeS₂	17–10–05	–	–	–	–	**34.078**	0.020	0.078	**30.492**	0.067	0.040	–	–	0.006	**33.728**	0.014	0.034	98.557
	17–10–06	0.013	–	0.013	0.008	**34.095**	0.190	0.061	**30.292**	–	0.033	–	–	–	33.654	–	0.054	98.413
Pyrite FeS₂	16–15–01	–	–	–	0.003	**53.203**	0.004	0.137	**46.646**	0.112	0.074	0.059	–	–	–	–	–	100.24
Galena PbS	17–10–07	–	–	–	0.008	**14.835**	0.537	**79.273**	4.973	0.346	–	–	0.019	–	0.026	0.082	–	100.09
	16–15–02	–	–	–	0.027	**13.345**	0.099	**84.982**	1.736	0.553	–	0.093	0.001	–	–	0.139	0.009	100.98
Chalcopyrite CuFeS₂	16–15–03	–	0.103	–	0.020	**34.342**	–	0.120	**30.084**	0.054	0.050	0.036	–	0.005	**34.309**	0.139	0.009	99.155
Pyrite FeS₂	16–2–01	0.063	–	0.039	0.002	**53.143**	–	0.162	**46.799**	–	0.067	0.023	–	–	–	–	–	100.29
	17–14–01	0.006	0.005	–	0.004	**52.907**	0.022	0.105	**46.517**	–	0.068	0.045	0.010	–	0.001	–	–	99.690
Altaite PbTe	17–14–02	–	–	**3.708**	–	0.223	0.163	**54.782**	1.575	0.415	–	**0.843**	–	0.277	0.035	**39.552**	0.019	101.59
Calaverite AuTe₂ or (Au, Ag)Te₂	17–14–03	–	–	**42.656**	0.014	0.762	–	–	2.373	0.267	–	**0.696**	–	0.433	0.453	**54.868**	–	102.52
	17–14–04	–	–	**43.330**	–	0.087	0.007	–	1.054	0.269	0.013	**0.662**	–	0.401	0.076	**56.313**	0.026	102.23
	17–16–01	–	–	**41.199**	0.013	0.155	0.013	–	0.830	0.308	–	**0.510**	–	0.425	–	**57.428**	–	100.88
Pyrite FeS₂	17–16–02	–	–	0.038	–	**53.162**	0.018	0.172	**46.332**	0.049	0.082	–	–	0.022	–	0.001	–	99.88
Average		0.005	0.008	13.04	0.006	21.101	0.176	25.150	17.312	0.203	0.029	3.566	0.007	0.096	3.940	14.734	0.011	99.358
Sigma		0.013	0.024	24.949	0.008	**22.357**	0.351	35.975	**20.248**	0.167	0.032	11.431	0.011	0.146	11.034	21.428	0.019	3.793

3.2. *Fluid inclusion analysis*

Fluid inclusions were analyzed in Key Laboratory of Geological Processes and Mineral Resources at China University of Geosciences (Wuhan) using a LinkamGP 600 heating-freezing system mounted on an Olympus-BX51 microscope. The image is transmitted to a monitor via a high-resolution Hamamatsu IRTV camera with a tube that has a maximal detection capability of about 2.2 μm. The micrographs were taken by a monitor QIMAGING MP5.0 cooled RTV under polarized light and U-V light. Uncertainties of the measurements are ± 0.5°, ± 0.2°, and ± 2°C for runs in the ranges of −120° to −70°, −70° to 100°, and 100° to 600°C, respectively. The heating/freezing rate was generally 0.2° to

5 °C/min, but was reduced to less than 0.2°C/min near the phase transformation. Primary fluid inclusion in the vein quartz are (L_w + V) and (L_w + L_{CO_2} + V), with NaCl+H_2O composition (Figure 5). These measurements include ice melting temperature ($T_{m, ice}$), clathrate melting temperature ($T_{m, clat}$), CO_2 homogenization temperature (T_h, CO_2), and total homogenization temperature (T_h) (Figures 5, 6).
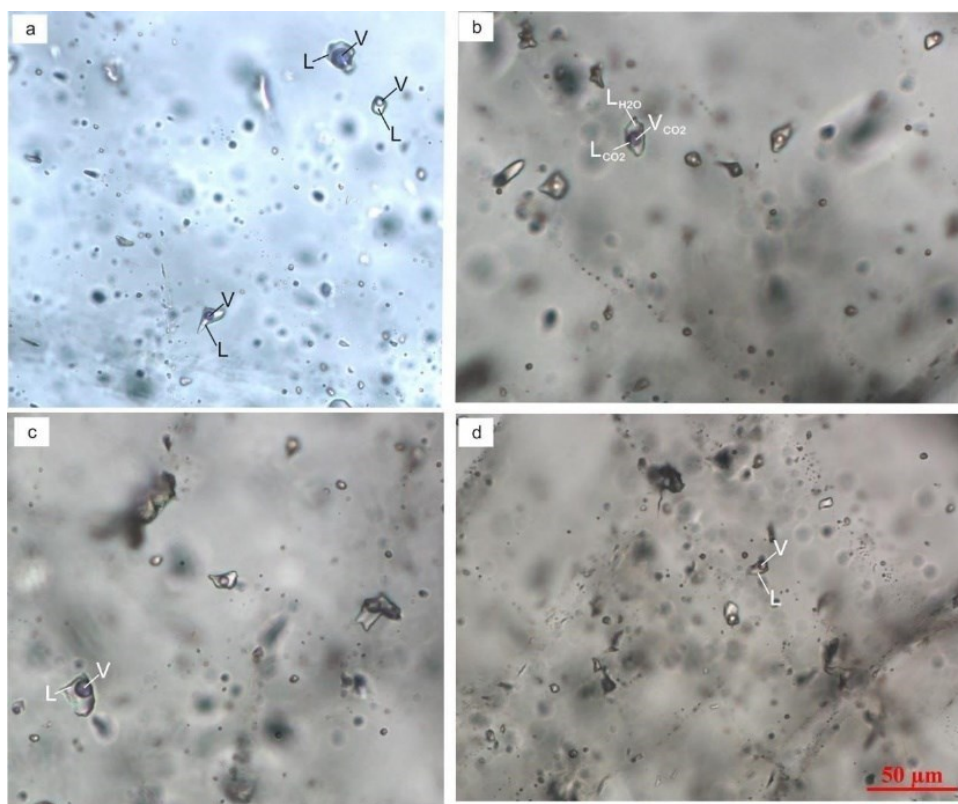
Fig. 5. Primary fluid inclusion assemblage in vein quartz is showing in the figure (L_{H_2O} + V) and (L_{H_2O}+L_{CO_2}+V)
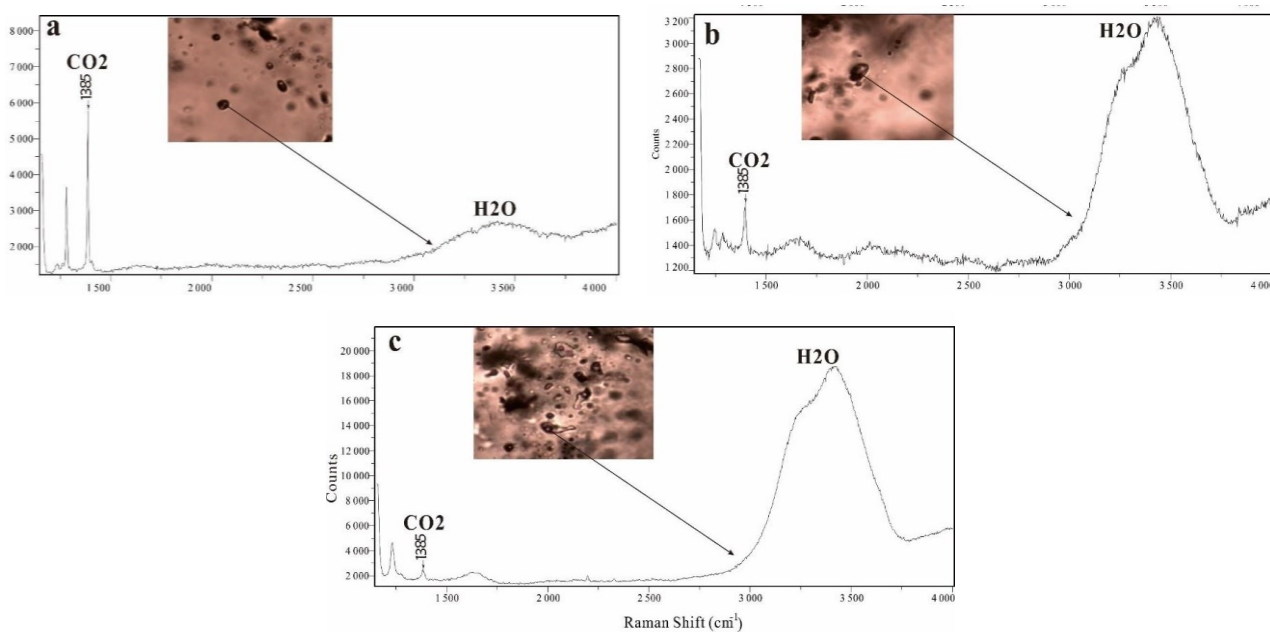
Fig. 6. Raman spectra of the two types of inclusions in quartz veins. (a) and (b-c) show coexisting CO_2 and H_2O in inclusions. The photomicrographs of fluid inclusion types from mineralized vein quartz, mainly L-V and L_{CO_2}-L_{H_2O}-V_{CO_2} types, all sizes ranging from 8 to 20 μm

3.3. *Oxygen and hydrogen isotopes*

The hydrogen and oxygen isotopes were analyzed in the Stable Isotope Laboratory of Mineral Resources Institute, Chinese Academy of Geological Sciences, using the Finnigan MAT253 mass spectrometer. Seven quartz samples from veins of different stages were analyzed. Oxygen was liberated from quartz by a reaction with BrF_5 and converted to CO_2 on a platinum-coated carbon rod for oxygen isotope analysis. The water of the fluid inclusions in quartz was released by heating the samples to above 500 °C by means of an induction furnace, and then reacted with zinc powder at 410 °C to generate hydrogen for isotope analysis. The results of oxygen isotope ratios are reported in per mil relative to Vienna Standard Mean Ocean Water (V-SMOW), with analytical uncertainty (1σ) of ±3 ‰ for δ^2H and ±0.2 ‰ for $\delta^{18}O$.

3.4. *Sulphur isotopes*

Sulphur isotopes of pyrite were determined using the direct oxidation method. Approximately 15 mg of sulfide was homogenized with 150 mg of Cu_2O, then combusted at 1,050°C for 15 min under vacuum for a quantitative conversion to sulphur dioxide (SO_2), which was analyzed for sulphur isotope composition on a MAT 230 mass spectrometer. Sulphur isotope ratios are expressed as per mil deviations from the sulphur isotope composition of Vienna Canon Diablo Troilite (V-CDT) using the conventional delta notation. Sulphur isotope results

are generally reproducible within ±0.2 ‰. The results of the previous and this study are presented in (Figure 7).
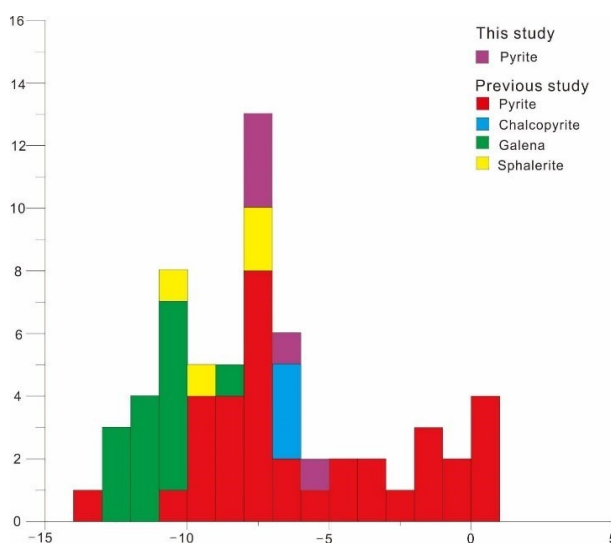
Fig. 7. Sulphur isotopic compositions of sulfide minerals in the Dongping gold deposit

3.5. *$^{40}Ar/^{39}Ar$ dating*

After the argon dating prerequisites in other laboratories of Guangzhou Institute of Geochemistry, Chinese Academy of Sciences and Chengdu in China. The final analysis for $^{40}Ar/^{39}Ar$ dating has been carrying out at the Key Laboratory of Tectonic and Petroleum Resources (China University of Geosciences – Wuhan), Ministry of Education, China.

4. RESULTS

4.1. *Ore telluride composition*

The gold ore at Dongping is closely associated with sulfide minerals in granitoids, invisible for optical observation and back-scattered electron imaging (BSE). The most important ore is native gold, which is commonly admixed with silver and copper (Table 2). Among the gold-bearing minerals tellurides contain significant gold, with exception of altaite, which tends to be gold-poor. Petzite (Ag, Au)$_2$Te, contains on average 19–23% Au, 38–46% Ag, and 32–35% Te, and calaverite (Au,Ag)Te$_2$, contains on average ~43% Au. The gold-bearing sulfides and tellurides are product of primary formation, although auriferous chalcopyrite might also be formed by secondary enrichment processes. Native gold may occur in the primary (white Quartz-K-feldspar-Pyrite) or secondary enrichment.

Telluride association occur at the third stage of mineralization (gold polymetallic sulfide-telluride-(grayish-white) quartz.

4.2. *Fluid inclusions and Raman spectrometry*

Fluid inclusions of previous studies in the deposit are in accordance with our data (Figure 6) what suggests that the deposit was formed during two main episodes of homogenization temperature. The first stage fluids with low temperatures (240 to 120°C) have corresponding salinities from 1.6 to 11.9 wt % NaCl equ. (average 6.04), determined by the ice and clathrate melting temperature (between –12 and 0°C). The second phase of fluid inclusions has higher homogenization temperature between 400 to 240°C and corresponding low salinities with average of 8.8 wt% NaCl equ.

T a b l e 2

LA-ICP-MS U-Pb zircon results of the samples DP-13 from the granite rocks in Dongping orebody

Spots	Th ppm	U ppm	Th/U Ratio	$^{207}Pb/^{206}Pb$ Ratio	$^{207}Pb/^{206}Pb$ 1sigma	$^{207}Pb/^{235}U$ Ratio	$^{207}Pb/^{235}U$ 1sigma	$^{206}Pb/^{238}U$ Ratio	$^{206}Pb/^{238}U$ 1sigma	$^{207}Pb/^{206}Pb$ Age (Ma)	$^{207}Pb/^{206}Pb$ 1sigma	$^{207}Pb/^{235}U$ Age (Ma)	$^{207}Pb/^{235}U$ 1sigma	$^{206}Pb/^{238}U$ Age (Ma)	$^{206}Pb/^{238}U$ 1sigma	Conc., %
DP13-1	961	1531	0.63	0.0481	0.0012	0.1498	0.0041	0.0224	0.0002	101.9	59.3	142	3.7	143	1.5	99
DP13-2	871	1445	0.60	0.0531	0.0014	0.1665	0.0047	0.0226	0.0002	345	61.1	156	4.1	144	1.4	91
DP13-6	1031	2037	0.51	0.0503	0.0015	0.1552	0.0050	0.0222	0.0003	206	38.0	147	4.4	142	1.7	96
DP13-7	1018	1789	0.57	0.0493	0.0016	0.1516	0.0052	0.0222	0.0003	165	74.1	143	4.6	141	1.9	98
DP13-8	969	1223	0.79	0.0493	0.0016	0.1555	0.0053	0.0227	0.0002	161	75.9	147	4.7	145	1.5	98
DP13-9	1051	1163	0.90	0.0500	0.0015	0.1597	0.0050	0.0231	0.0003	195	70.4	150	4.4	147	1.8	97
DP13-10	699	863	0.81	0.0488	0.0019	0.1543	0.0062	0.0229	0.0003	200	92.6	146	5.4	146	1.8	99
DP13-11	786	961	0.82	0.0510	0.0020	0.1607	0.0057	0.0231	0.0003	239	90.7	151	5.0	147	1.9	97
DP13-12	761	859	0.89	0.0484	0.0019	0.1510	0.0060	0.0225	0.0002	120	88.0	143	5.3	144	1.5	99
DP13-14	1335	2588	0.52	0.0507	0.0013	0.1551	0.0039	0.0221	0.0002	233	59.2	146	3.4	141	1.5	96
DP13-15	1400	2806	0.50	0.0490	0.0012	0.1495	0.0035	0.0221	0.0002	146	62.0	142	3.1	141	1.1	99
DP13-16	2343	3570	0.66	0.0541	0.0013	0.1684	0.0040	0.0224	0.0002	376	56.5	158	3.5	143	1.2	89
DP13-17	1383	2316	0.60	0.0519	0.0014	0.1587	0.0043	0.0221	0.0002	280	63.0	150	3.8	141	1.2	93
DP13-18	637	953	0.67	0.0481	0.0019	0.1524	0.0061	0.0229	0.0003	101.9	92.6	144	5.4	146	1.9	98
DP13-19	611	1177	0.52	0.0526	0.0019	0.1663	0.0057	0.0230	0.0003	322	81.5	156	4.9	146	1.7	93
DP13-20	1097	2442	0.45	0.0522	0.0015	0.1592	0.0042	0.0221	0.0002	295	67.6	150	3.7	141	1.3	93
DP13-22	972	1102	0.88	0.0493	0.0016	0.1541	0.0048	0.0227	0.0003	165	77.8	145	4.3	145	1.9	99
DP13-23	831	932	0.89	0.0480	0.0018	0.1503	0.0056	0.0227	0.0003	102	88.9	142	4.9	145	1.7	98
DP13-25	736	1000	0.74	0.0492	0.0019	0.1550	0.0059	0.0227	0.0002	167	88.9	146	5.2	144	1.5	98
DP13-26	1976	3067	0.64	0.0513	0.0013	0.1567	0.0042	0.0219	0.0003	257	62.0	148	3.7	140	1.6	94
DP13-27	540	574	0.94	0.0535	0.0024	0.1644	0.0073	0.0223	0.0003	346	106	155	6.4	142	1.6	91
DP13-28	1040	1787	0.58	0.0490	0.0013	0.1551	0.0046	0.0227	0.0003	150	61.1	146	4.0	145	1.7	98
DP13-30	890	1249	0.71	0.0497	0.0014	0.1554	0.0045	0.0226	0.0002	189	60.2	147	3.9	144	1.5	98

These results on the Dongping gold deposit are consistent with data of other studies on fluid inclusions in the deposit (Zhang & Mao, 1995; Nie, 1998; Fan et al., 2001; Mao & Li, 2001; Mao et al., 2003; Zhang et al., 2012). Bao et al. (2015), indicated the ore forming fluids have the following characteristics (low salinity ranging from 0.7 to 8.1% wt. NaCl equ., homogenization temperatures of 310 to 350° C and the chemical composition of fluids are H_2O-CO_2-NaCl.

Results of Raman spectroscopy confirm that CO_2 and H_2O are the main volatiles, accompanied by small amounts of N_2, H_2S, CH_4, C_2H_2 and CO (Mao et al., 2003).

The presence of H_2O-CO_2 inclusions, which contain both liquid and vapor CO_2 are commonly produced in a deep environment, what eliminates epithermal mineralization as a potential genetic model. The fluid inclusions data provide a strong argument in favor of a magmatic source of the hydrothermal fluids and possible mixing with variable amounts of meteoric water (Figure 8).

4.3. *Isotope geochemistry*

The sulfides from the Dongping deposit and the other gold deposits related to the Shuiquangou syenite intrusion have variable $\delta^{34}S$ values, which may have resulted from different sulphur sources and/or distinct oxygen fugacities. These results of the previous studies, Song & Zhao, (1996); Nie, (1998); Wang et al., (1990); Hart et al., (2002); and

this study ($\delta^{34}S$ = –7.3 to –5.6 ‰,VCDT) are presented in the plot Figure 8. The results for oxygen in vein quartz and hydrogen in fluid inclusion in this study range from +3.85 to +4.78 ‰ ($\delta^{18}O_{quartz}$) and –100.3 to –74.7 ‰ ($\delta^2H_{fluid\ inclusion}$, all values relative to VSMOW). The published results in the Figure 8 by Bao et al. (2015), ($\delta^{18}O_{quartz}$ ranging from –1.7 to + 6.9 ‰ and $\delta^2H_{fluid\ inclusion}$ values of –108 to –66.5 ‰, average of –85 ‰) are equivalent to our analysis but we assume a slight different interpretation. The calculated oxygen isotope composition of the fluid for this study varies between +3.38 to +4.78 ‰. The analyses of H-isotopic composition, measured directly on fluid inclusions are in the plot of δ^2H vs. $\delta^{18}O$ (Figure 9). Quartz samples fall in the zone of "organic water" between the magmatic water field and the meteoric line. The Dongping Au deposit shares many features in common with gold deposits Pengjiakuang, Pai,

from the same craton in NCC, and mesothermal lode gold deposit model in green schist facies environments is not *a priori* refused. The possible ore-forming fluid in the Dongping gold deposit may be a mixture of water derived by organics and mag water, but deep seated brines, equilibrated with the host rocks, could have participated as well.

The $^{87}Sr/^{86}Sr$ of Dongping range from 0.7006 to 0.7060 similar to the value of East China igneous rock (0.702215 – 0.704300). In contrast, rocks of Shanshuiquan have higher $^{87}Sr/^{86}Sr$ values between 0.706019 and 0.708976 (Bao et al., 2015; Jiang et al., 2009). Thus, the two appear to have distinct sources according to the $^{86}Sr/^{86}Sr$ isotope ratios. This diagram also points to possible complex associations of fluids important for the genesis, "meteoric, evolved meteoric and magmatic type" (Figure 9, diagram after Norman & Landis, 1983).
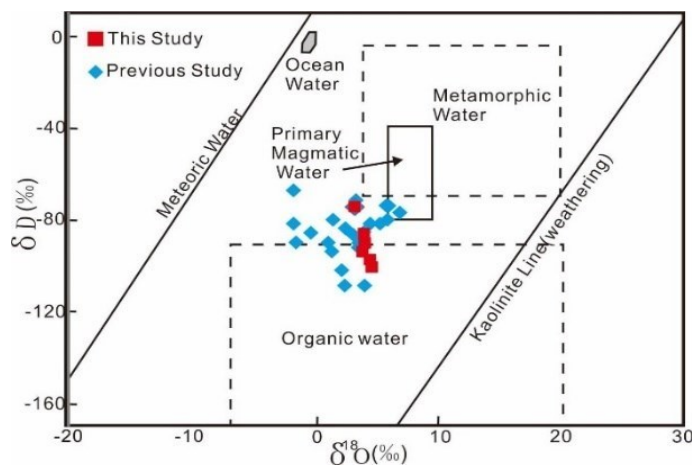
Fig. 8. Hydrogen and oxygen isotopic compositions of ore-forming fluids from the Dongping gold deposit. Isotopic composition of ore-forming fluid in equilibria with the vein quartz was calculated by the following relation: $\delta^{18}O_{fluid} = \delta^{18}O_{quartz}$ $(4.48 \times 10^6) / T^2 – 4.47 \times 10^3 / T + 1.71$. (Diagram modified from White, 1974; Sheppard, 1986)
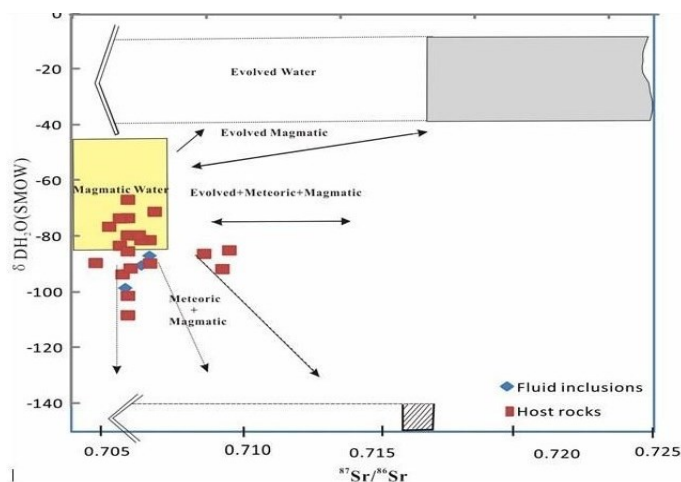
Fig. 9. Plot of the independent variables δ^2H and $^{87}Sr/^{86}Sr$ ratio illustrating the component mixture of hydrothermal fluids (after Norman & Landis, 1983)

4.4. $^{40}Ar/^{39}Ar$ dating

The two K-feldspar from altered syenite samples analyzed by $^{40}Ar/^{39}Ar$ *in vacuo* crushing yield complicated age spectra, which could have been disturbed by post geological events, starting with abnormally old apparent ages that decrease rapidly in several steps, to flat age plateaus in the final steps (Figure 10). The abnormally old ages observed in the first crushing steps may be caused by the release of trapped excess ^{40}Ar from the much

larger primary inclusions containing a hydrothermal gas phase originating from the magma chamber. The plateau ages obtained in the final crushing steps of these two K-feldspar samples are, respectively, 154.89 ± 0.70 Ma, Total Fusion 146.10 ± 0.29, Normal Isochron 153.92 ± 3.72, Inverse Isochron 154.13 ± 3.72 Ma and 176.93 ± 4.66 Ma, Total Fusion 146.10 ± 0.29, Normal Isochron 153.92 ± 3.72 Ma, Inverse Isochron 251.77 ± 206.35 Ma. The other parameters of $^{40}Ar/^{39}Ar$ are presented in the Figure 10.
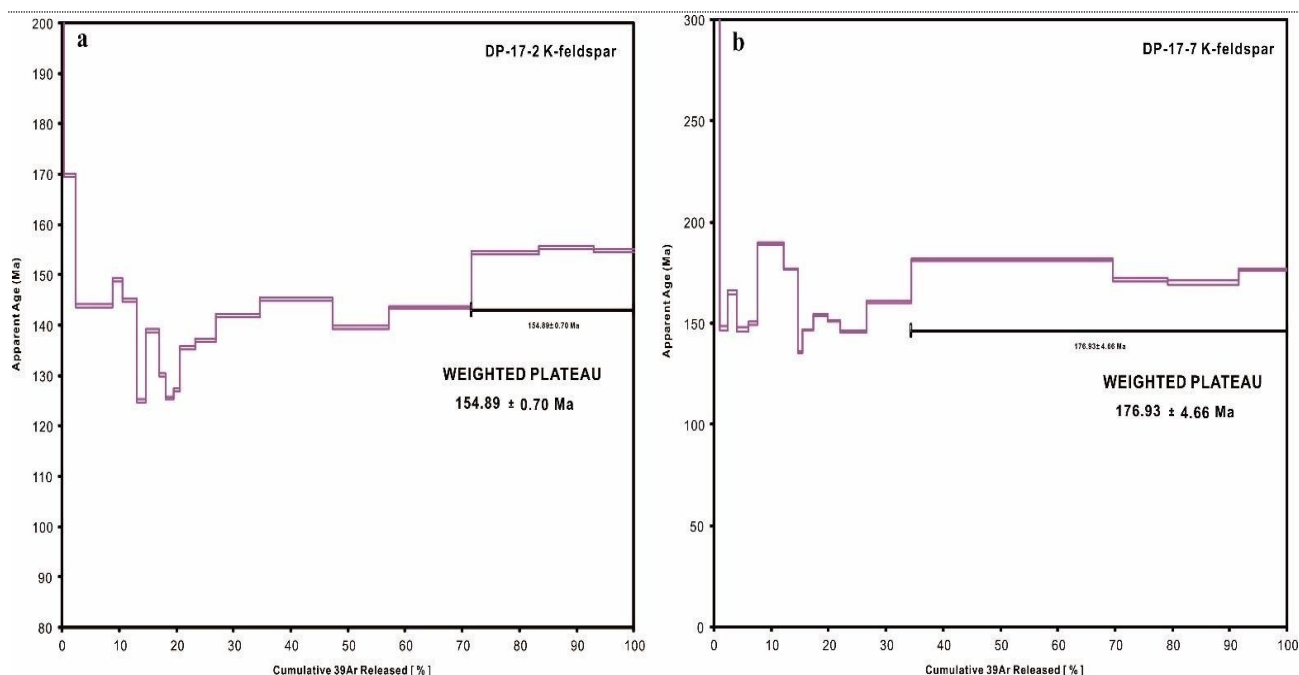
Fig.10. Laser incremental heating $^{40}Ar/^{39}Ar$ age spectra of two K-feldspar samples (a and b) by in vacuo crushing, showing consistent weighted plateau ages

5. DISCUSSION

5.1. *Ore minerals and style of mineralization*

The ores in Dongping are telluride-rich and sulfide-poor (<2%) (Song & Zhao, 1996). The tellurides in the ore are scattered as micron-sized grains among the other ore minerals. Previous studies have identified electrum, calaverite, petzite, altaite, sylvanite, krennerite, hessite, tellurobismuthite, tetradymite and stutzite in the auriferous quartz veins from the upper parts of the ore bodies (Song & Zhao, 1996; Zhang et al., 2002 ; Gao et al., 2014). The average ratio of telluride to gold is 0.71, and this ratio increases with gold grade (Zhang et al., 2001). The gold-bearing zones are consistently associated with tellurium-bearing calaverite (Zhang & Mao, 1995). All previous research on the Dongping gold deposits has inferred that they are

spatially and genetically related to the Shuiquangou alkaline complex.

5.2. *Source of ore-forming fluid*

The Shuiquangou syenites may have been the principal sulfur source for the ore-forming fluids. Reported $\delta^{34}S$ values have been shown to be as low as −20 and as high as +25‰ for sulfide minerals from orogenic gold deposits, but very negative $\delta^{34}S$ data indicate a non-mantle sulfur source (Goldfarb et al., 2015). The negative sulfur isotope values suggest that it is an orogenic gold deposit of magmatic origin (Figure 7). Dongping and Wulashan have similar sulfur isotope signatures with no sulphate minerals (Nie and Bjorlykke. 1994). The

pyrites from the gold deposits related to the syenite complex have S^{34} positive values indicating a magmatic origin (Figure 7).

The interpretation of previous results and the data from this study show that the source of sulphur isotopes (Figure 7) is magmatic, whereas oxygen and hydrogen isotopes of the ore-forming fluids plot mainly in the zone of primary magmatic water mixed with organic water and meteoric water (Figure 8). Mixing of the meteoric water and magmatic fluids caused cooling, and dilution of the magmatic-hydrothermal fluid. This may have led to precipitation of native gold, electrum, calaverite, and altaite.

The $^{87}Sr/^{86}Sr$ of Dongping range from 0.7006 to 0.7060 similar to the value of East China igneous rock (0.702215 – 0.704300) and Shanshuiquan with high $^{87}Sr/^{86}Sr$ values between 0.706019 and 0.708976 (Figure 9), indicate depleted mantle, respectively, or frequently observed prevalent mantle composition in the mantle xenoliths (sub-continental lithosphere) (Song & Fray, 1998), and a source from subduction-related volcanic rocks (young volcanic-arc) (McDermott & Hawkesworth, 1991). The δ^2H_{H2O} versus $^{87}Sr/^{86}Sr$ isotope ratios show also the composite water source of the fluids; magmatic + meteoric + evolved, leached from igneous rocks by non magmatic fluids.

5.3. *Ages of host rocks and gold mineralization*

There has been extensive debate about the origin of these deposits, and specifically the age of mineralization and relationship to the host rocks. The last magmatism in the region is identified by the emplacement of the Shangshuiquan granitic pluton during the Early Cretaceous (ca. 140 Ma), which temporally coincided with the Yanshanian Orogeny (Miao et al., 2002; Cissé et al., 2017).

This orogenic event was characterized by rifting linked to widespread Jurassic–Cretaceous terrestrial volcanism and granite intrusion in eastern China (Chang et al., 1994; Tian et al., 1992; Miao et al., 2002). Early Cretaceous magmatism was widespread in this region, as shown by emplacement of the Zhuanzhilian diorite at 139.5±0.9 Ma (Jiang et al., 2007). The Yanshanian event was probably the most productive in terms of mineral systems and is considered by most authors to be related to delamination of the lithospheric mantle, resulting in magmatic underplating, crustal melting and the development of A- and I-type granitic magmas and volcanism along the East Asian margin in rift

structures. Giant and world-class mineral systems all formed during the Yanshanian in eastern China (Pirajno, 2013).

Cisse et al. (2017) by zircon dating showed that there are two periods of magmatism with distinctly different ages in the Shuiquangou igneous complex (Dongping district). Emplacement of the host syenites/quartz syenites took place at 394.0 ± 3.2 Ma and coeval mafic–ultramafic complexes (395 to 390 Ma) have been identified in the western and central parts of the region, consistent with the known tectonic history in the region (Zhang et al., 2005).

In contrast, the alkali granites, which are temporally related to the mineralization in the Dongping deposit, were intruded at 143±1 Ma. The dated zircons in the Cisse et al. (2017) study have Th and U concentrations averaging about 1880 ppm and 2957 ppm, respectively, yielding an average Th/U ratio of 0.59, indicating a magmatic origin. All of the zircons have significantly negative εHf(t) values ranging from –25.8 to –16.9 indicating that pre-existing continental crust was involved in the formation of the magmas, consistent with a crustal derivation of magmas in other parts of the NCC (Zhang et al., 2012). These values of εHf(t) do not rule out a small contribution from a lower crustal lithologies. Various studies have demonstrated that U-Pb dating of hydrothermal zircon from altered rocks (K-feldspar granite) and quartz veins of ore deposits is an appropriate tool for determining the age of ore formation (Kerrich & King, 2003; Peller et al., 2007; Zartman & Smith, 2009). Thus, we conclude that the mineralization in the Dongping deposit was most likely related to emplacement of the alkali granites at ca. 143 Ma. Some early mineralization may have been associated with intrusion of the syenites/quartz syenite of the Shuiquangou complex (Bao et al., 2015).

Due to the complexity and size of the gold deposit located in the NCC, it is possible that there were several episodes of mineralization. The main stage of mineralization took place in the latest Jurassic to Early Cretaceous, which corresponds to the Yanshanian orogenic event in the study region. We infer that there were multiple magmatic/hydrothermal events over a range of some millions of years during the Late Jurassic to Early Cretaceous.

Zircon dating in this study confirmed the age determination in the former research (Cisse et al., 2017), and brought evidence of thermal history of the ore formation. Radiometric dating studies were carried out by LA-ICP-MS U-Pb at the State Key

Laboratory of Geological Processes and Mineral Resources of the China University of Geosciences (Wuhan).

5.4. *Gold mineralization process*

Characteristics of fluid inclusions (Figures 5, 6) suggests that the deposit was formed during two prominant episodes. These two stages generated mineral association are related with tellurides in Dongping gold deposit. The first stage with fluids between 240 to 400°C and corresponding low Salinities (average of 8.8 wt% NaCl equ.). The second stage with fluids of low to moderate temperatures (240 to 120°C) and corresponding salinities from 1.6 to 11.9 wt % NaCl equ. (average 6.04).

The recent dating (inverse isochron 154.13 ± 3.72 Ma and 176.93 ± 4.66 Ma) by the Ar/Ar method confirms, two-episode model of mineralization at Jurassic/Cretaceous events in line with previous data.

Interpretation of genesis requires concert of all achieved data, and dynamics of temporal and spatial geochemical variability in the deposit. Gold mineralization, its character and paragenesis reflects physico-chemical evolution of fluids. The early ore forming fluids were magmatic, metamorphogenic, named "evolved water" equilibrated with the host rocks, and receiving their isotope signature of Landis (1983). The granitic intrusion introduced pervasive alteration of syenitic granitoids by water with low pH, releasing colloidal silica, followed by voluminous K-feldspathitization, and pyritization. The gold was transported as bisulfide complexes $Au(HS)_2^-$ and $HAu(HS)_2^o$ and deposited by chemical reaction path proposed by Hofstra et al. (1991), caused by intrusion and dilution with meteoric oxygenated waters, drop in temperature and sulfidization of the host syenitic rocks.

$$Au(HS)_2^- + FeO + H^+ = FeS_2 + Au^o + H_2O + 1/2H_2$$
$$(1)$$
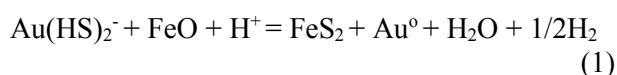
The gold was deposited with base-sulfides, pyrite, chalcopyrite, sphalerite, galena and tetrahedrite. A side effect of leaching syenitic rocks is release of characteristric metal association that includes Bi, As, and Te, and lesser amounts of Sn, Zn, Cr, Pt, Cu, Pb and Sb.

Intrusion of oxygenated waters is recognized by some side effects, like deposition of accessory minerals, magnetite, hematite and barite. Oxidizing condition pushed the $\delta^{34}S$ values of sulfides from zero and slightly positive, to –14 ‰. Oxidation of sedimentary organic matter generated abundant CO_2 in the system, and contributed to the isotope patterns of D/O in water (Figure 8).

Besides, drop of $f(S_2)$ increased relative value of $f(Te_2)$ inevitably, and initiated wide spread deposition of tellurides. Telluride precipitation requires high tellurium fugacity and low sulphur fugacity (Song & Zhao, 1996). It is supported by the negative correlation between sulfides and tellurides in the deposit. The tellurides postdate sulfides in a sulphur depleted environment, as a result of sulfide precipitation (Tu et al., 2004). Incipient telluride precipitation incorporated Pb to form altaite, followed by Au and Ag in petzite. Exhaustion of Ag prefers incorporation of Au in calaverite, and finally Au as native gold formed from the residue (Shen et al., 2015). The final result is very heterogeneous distribution of telluride species and their concentration all over the ore deposit. Cooling of the system enhance fracturing, penetration of meteoric water and massive oxidation of sulfides, limonitization, and supergene enrichment of very pure gold (98 wt. %).

5.5. *Gold deposit type*

Taking into account the characteristics of ore-forming environments and key features of the deposit described above: such as CO_2 rich, low salinity, fluid temperatures, partial melting of deep crust in Archean (± Paleoproterozoic) basement in NCC, and pre-existing faults, accumulation of gold bearing veins or zones of disseminated sulfide, and Au>Ag, a metal assemblage that includes Bi, As, and Te, and lesser amounts of Zn, Pb, Cu and Sb, the deposit is best classified as an "intrusion gold deposit" of magmatic origin (Sillitoe, 2008), rather than "orogenic model" which is less constrained to the presented circumstances (Goldfarb et al., 2001, 2005, 2007, 2015). The low-salinity, CO_2-rich ore-fluids reflect influence of deep seeted fluids of metamorphogenic hydrothermal origin, driven by heat of magma intrusion, which is typical of most "intrusion gold deposits" (Miller et al., 1998). The late timing of gold mineralization with respect to felsic magmatism in the Dongping ore-field is similar to that observed elsewhere in North China, as in the Jiaodong Peninsula, Xiaoqiling (Wang et al., 1998; Hua & Mao, 1999). Closure of the Paleo-Asian Ocean at the end of the Permian and continued convergence from the north during the Triassic to Early Jurassic led to post-collisional thrusting and considerable crustal thickening on the northwestern side of the North China Craton (Xiao et al., 2003).

The ore fluid geochemistry, ore and alteration mineralogy, the absence of auriferous sheeted ore veins and the structural setting of the ores, led us to classify this deposit as "intrusion gold deposits" of complex hydrothermal origin, with water of magmatic, meteoric and organic origins, in the category of gold deposit with stockworks, disseminated and vein gold mineralization in the northern margin of the North China Craton.

6. CONCLUSION

The Dongping gold deposit is hosted by the Shuiquangou alkaline complex, which consists mainly of monzonite, quartz monzonite, and aegirine syenite**.** Most gold resides in telluride minerals, of which the most abundant are calaverite, petzite and altaite. The type of gold ore is classified according to its mineral association as quartzose gold, telluride gold or disseminated gold. Wall rock alteration accompanying gold mineralization is mainly potassic (K-feldspar) and silicic in proximity to veins; more distally, sodic (albite), (calcite), sericitic and epidotic alteration are important.

The fluid inclusion data display two ranges of homogenization temperature, the majority from 240 to 400ºC (avg. 306ºC) and the remainder from 240 to 120ºC. These inclusions are characterized by the CO_2^- rich and low salinity fluids, respectively, with 6.04 and 8.8 wt% NaCl equ. The Raman data evidence mainly H_2O and CO_2 compositions.

The weighted plateau $^{40}Ar/^{39}Ar$ ages from two K-feldspar samples yielded 154.89 ± 0.70 Ma and 176.93 ± 4.66 Ma, showing two stage of mineralization in the deposit.

The Dongping gold deposit is classified as an intrusion gold deposit according to the following features: (1) formation within the continental margins at NCC (i.e. occurring in the central part of the Shuiquangou syenite); (2) a genetic relationship to felsic intrusions; (3) a metal association that includes Bi, As and Te, and lesser amounts of Sn, Zn, Cr, Pt, Cu, Pb and Sb; (4) a reduced sulfide mineral assemblage mainly consisting of pyrite; (5) a low sulfide mineral content; (6) the timing of gold mineralization emplacement related to Yanshan orogeny; (7) wallrock alteration characterized by inner K-feldspar-quartz-sericite facies and outer propylitic facies, and (8) CO_2-rich hydrothermal fluids of low salinity.

REFERENCES

Bao, Z. W., Zhao, Z. H., Zhang, P. H., Wang, Y. X. (2003): REE, Sr, Nd, and Pb isotopic evidence for the petrogenesis of the Shuiquangou syenite complex in NW Hebei Province China, *Geology Review*, **49**, 621–627 (in Chinese with English abstract).

Bao, Z. W., Zhao, Z. H. (2006): Isotopic Geochemical constraints on metallogeny of the Dongping–type gold deposits associated with syenites, *Acta Petrologica Sinica*, **22**, 2534–2542 (in Chinese with English abstract).

Bao, Z. W., Sun, W. D., Li, C. J., Zhao, Z. H. (2014): U-Pb dating of hydrothermal zircon from the Dongping gold deposit in north China: Constraints on the mineralization processes, *Ore Geology Reviews*, 61, 107–119.

Bao, Z. W., Li, C. J., Zhao, Z. H. (2015): Metallogeny of the syenite-related Dongping gold deposit in the northern part of the North China Craton: a review and synthesis, *Ore Geology Reviews*, 73, 198–210.

Chang, E. Z., Ying, X. D., Zhou, A., Wang, L. B. (1994): Geodynamic evolution of continental margins in Eastern Asia and tectonic setting of East China Sea In: Coleman, R. G (Ed.), Reconstruction of the Paleo-Asian Ocean, *Proc 29th Int Geol Congress*, Part B, pp. 133–167.

Chen, J. H. (2006): *Chongli County, Hebei Province, Dongping Goldfields 70.3 vein detailed investigation of geological reports* Internal report of Zijin Mining Group Co Ltd (unpublished data).

Cisse, M., Xinbiao, L. V., Algeo, T. J., Cao, X., Wei Mei, Yuan, Q., Mao, C., Huan, Li. (2017): Geochronology and geochemical characteristics of the Dongping ore – bearing granite, NE China: sources and implications for its tectonic setting, *Ore Geology Reviews*, **89**, 1091–1106.

Cook, N. J., Ciobanu, C. L., Mao, J. W. (2009): Textural control on gold distribution in As-free pyrite from the Dongping, Huangtuliang and Hougou gold deposits, North China Craton (Hebei Province, China), *Chemical Geology*, **264**, 101–121.

Diwu, C. R., Sun, Y., Wang, Q. (2012): The crustal growth and evolution of North China craton revealed by Hf isotopes in detrital zircons from modern rivers, *Acta Petrologica Sinica*, **28**, 3520–3530.

Fan, H. R., Xie, Y. H., Zhai, M. G. (2001): Ore-forming fluids in the Dongping gold deposit, northwestern Hebei Province Science in China D: *Earth Sciences*, **44**, 748–757.

Gao, S., Rudnick, R. L., Carlson, R. W., Mcdonough, W. F., Liu, Y. S. (2002): Re–Os evidence for replacement of

ancient mantle lithosphere beneath the North China craton. *Earth and Planetary Science Letters*, **198**, 307–322.

Gao, S., Xu, H., Zhang, D. S., Shao, H. N., Quan, S. L. (2014): Ore petrography and chemistry of the tellurides from the Dongping gold deposit, Hebei Province, China, *Ore Geology Reviews*, **64**, 23–34.

Geng, Y. S., Du L., Ren, L. (2012): Growth and reworking of the early Precambrian continental crust in the North China Craton: constraints from zircon Hf isotopes, *Gondwana Research*, **21**, 517–529.

Goldfarb, R. J., Baker, T., Dube, B., Groves D. I., Hart, C. J. R., Gosselin, P. (2005): Distribution, Character, and Genesis of Gold Deposits in Metamorphic Terranes, *Economic Geology*, 100th Anniversary Volume, 407–450.

Goldfarb, R. J., Groves, D. I., Gardoll, S. (2001): Orogenic gold and geological time: a global synthesis, *Ore Geology Reviews*, **18**, 1–75.

Goldfarb, R. J., Hart, C., Davis, G., Groves, D. I. (2007): East Asian gold: deciphering the anomaly of Phanerozoic gold in Precambrian cratons, *Economic Geology*, **102**, 341–345.

Goldfarb, R. J., Richard, J., David, I., Groves, D. I. (2015): Orogenic gold: Common or evolving fluid and metal sources through time, *Lithos*, **233**, 2–26.

Hart, C. J. R., Goldfarb, R. J., Qiu, Y. M., Snee, L., Miller, L. D., Miller, M. L. (2002): Gold deposits of the northern margin of the North China Craton: multiple late Paleozoic-Mesozoic mineralizing events, *Mineralium Deposita*, **37**, 326–351.

Helt, K. M., Williams-Jones, A. E., Clark, J. R., Wing, B. A., Wares, R. P. (2014): Constraints on the genesis of the Archean oxidized, intrusion-related Canadian Malartic gold deposit, Quebec, *Canada Economic Geology*, **109**, 713–735.

Hofstra, A. H., Leventhal, H. R., Northtrop, G. P., Landis, R. O., Rye, D. J., & Birak, A. R. (1991): Genesis of sediment-hosted disseminated-gold deposits: chemical reaction path modeling depositional processes documented in the Jerritt Canyon district, *Nevada Geology*, **19**, 36–49.

Hu L., Song, H. L., Yan, D. P., Hu, D. G. (2003): The Ar/Ar geochronology constraint and geological significance of mylonites in Shangyi-Chicheng fault belt on the north of North China Craton, *Science China*, **Ser D 46**: 1134–1141.

Hua, R. M., Mao, J. W. (1999): A preliminary discussion on the Mesozoic metallogenic explosion in East China, *Mineral Deposits*, **18**, 301–308.

Jiang, N., Sun, S. H., Chu, X., Mizutab, T., Ishiyama, D. (2003): Mobilization and enrichment of high-field strength elements during late and post-magmatic processes in the Shuiquangou syenitic complex, Northern China, *Chemical Geology*, **200**, 117–128.

Jiang, N., Liu, Y. S., Zhou, W. G., Yang, J. H., Zhang, Q. (2007): Derivation of Mesozoic adakitic magmas from ancient lower crust in the North China craton, *Geochimica et Cosmochimica Acta*, **71**, 2591–2608.

Jiang, N., Zhang, S., Zhou, W., Liu, Y. (2009): Origin of a Mesozoic granite with A type characteristics from the North China Craton: highly fractionated from I-type magmas? *Contributions to Mineralogy and Petrology*, **158**, 113–130.

Kerrich, R., King, R. (1993): Hydrothermal zircon and baddeleyite. In: Val-d'Or Archean mesothermal gold deposits:

characteristics, compositions, and fluid-inclusion proprieties, with implications for timing of primary mineralization, *Canadian Journal of Earth Sciences*, **30**, 2334–2351.

Kröner, A., Wilde, S. A., Li, J. H., Wang, K. Y. (2005): Age and evolution of the late Archean to Paleoproterozoic upper to lower crustal section in the Wutaishan/Hengshan/Fuping terrain of Northern China, *Journal of Asian Earth Sciences*, **24**, 577–595.

Kusky, T. M., Windley, B. F., Zhai, M. G. (2007): Tectonic evolution of the North China Block: from orogen to craton to orogen, M. G. Zhai (Ed.), *Mesozoic Sub-Continental Lithospheric Thinning under Eastern Asia,* Geological Society Special Publications, 1–34.

Li, C. M. (1999): Relationship between the gold source of Dongping gold deposit and Archean TTG-greenstone belt. Prog, *Precambrian Research*, **22**, 40–46 (in Chinese with English abstract).

Li, C. M., Deng, J. F., Chen, L. H., Su, S. G, Li, H. M., Hu, S. L. (2010): Two periods of zircon from Dongping gold deposit in Zhangjiakou-Xuanhua area, northern margin of North China: constraints on metallogenic chronology, *Mineral Deposits,* **29**, 265–275 (in Chinese with English abstract).

Li, H., Watanabe, K., Yonezu, K. (2014a): Zircon morphology, geochronology and trace element geochemistry of the granites from the Huangshaping polymetallic deposit, South China; Implications for the magmatic evolution and mineralization processes, *Ore Geology Reviews*, **60**, 14–35.

Lu, D. L., Wang, J. J., Luo, X. Q., Zhang, S. H., Zheng, B. Y. (1993): Geochronological study on the Dongping gold deposit, *Mineral Deposits*, **12**, 182–188 (in Chinese with English abstract).

Lu, S. N., Li, H. K., Yang, C. L., Hu, Z. D., Jiang, M. M. (1997): *The Characteristics of Basements and Metallogenic Study of Gold Deposit Concentrated Areas*, Geology Publishing House, Beijing, China, 6–44 (in Chinese).

Luo, Z., Miao, L. Guan, K., Qiu, Y., Mcnaughton, N. J. (2001): SHRIMP chronological study of Shuiquangou intrusive body in Zhanjiakou area, Hebei Province and its geochemical significance, *Geochimica*, **30**, 116–122 (in Chinese).

Mao, J. W., Li, Y. Q. (2001): Fluid inclusions of the Dongping gold telluride deposit in Hebei Province, China: involvement of mantle fluid in metallogenesis, *Mineral Deposits*, **20**, 23–36 (in Chinese with English abstract).

Mao, J. W., Li, Y. Q., Goldfarb, R. J., He, Y., Zaw, K. (2003): Fluid inclusion and noble gas studies of the Dongping gold deposit, Hebei Province, China: a mantle connection for mineralization? *Economic Geology*, **98**, 517–534.

Mcdermott, F., Hawkesworth, C. J. (1991): Th, Pb and Sr isotopic variations in Young Island arc volcanic and oceanic sediments, *Earth and Planetary Science Letters,* **104**, 1–15.

Miao, L., Qiu, Y. M., Mcnaughton, N., Luo, Z. K., Groves, D., Zhai, Y. S., Fan, W. M., Zhai, M. G., Guan, K. (2002): SHRIMP U–Pb zircon geochronology of granitoids from Dongping area, Hebei Province, China: Constraints on tectonic evolution and geodynamic setting for gold metallogeny, *Ore Geology Reviews*, **19**, 187–204.

Miller, L. D., Goldfarb, R. J., Nie F. J., Hart, C. J. R., Miller, M. L., Yang, Y. Q., Liu, Y. Q. (1998): North China gold: A product of multiple orogens, *Society of Economic Geology Newsletters*, **33**, 1, 6–12.

Mo, C. H. (1996): *Geochemistry and metallogeny of gold deposits in Zhangjiakou area*, Ph.D. dissertation, Guangzhou Institute of Geochemistry, *Chin Acad Sci.*, 48 p (in Chinese with English abstract).

Nie, F. J., Wu, C. Y. (1995): Gold deposits related to alkaline igneous rocks in the North China Craton, People's Republic of China. In: *Mineral Deposits: From Their Origin to Their Environmental Impacts* (Pasava, J. et al., eds.), Proc. 3rd Biennial SGA Meet., Prague, 173–176, A. A. Balkema, Rotterdam.

Nie, F. J. (1998): Geology and origin of the Dongping alkalic-type gold deposit, Northern Hebei Province, People's Republic of China, *Resource Geology*, **48**, 139–158.

Nie, F. J., Jiang, S. H., Liu, Y. (2004): Intrusion-related gold deposits of North China Craton, People's Republic of China, *Resource Geology*, **54**, 299–324.

Norman, D. I.,, Landis, G. P. (1983): Source of mineralizing component in hydrothermal ore fluids as evidenced by $^{87}Sr^{86}Sr$ and stable isotope data from the Pasto Bueno deposit, *Peru Economic Geology*, **78**, 451–465.

Peller, E., Chelletz, A., Gasquet, D., Mouttaq, A., Annich, M., El Hakour, A., Deloule, E., Feraud, G. (2007): Hydrothermal zircons: A tool for ion microprobe U-Pb dating of gold mineralization (Tamlatt-Menhouhou gold deposit, Morrocco), *Chemical Geology*, **245**, 135–161.

Pirajno, F. (2013): *The Geology and Tectonic Settings of China's Mineral Deposits*, Springer, Perth, Western Australia, 689 pp.

Santosh, M. (2010): Assembling North China Craton within the Columbia supercontinent: the role of double-sided subduction, *Precambrian Research*, **178**, 149–167.

Santosh, M., Liu, D., Shi, Y., Liu, S. J. (2013): Paleoproterozoic accretionary orogenesis in the North China Craton: A SHRIMP zircon study, *Precambrian Research*, **227**, 29–54.

Shen, G., Hong, X. U., Desen, Z., Henan, S. & Shaolong Q. (2015): Ore petrography and chemistry of the tellurides from the Dongping gold deposit, Hebei Province, *China Ore Geology Reviews*, **64**, 23–34.

Sheppard, S. M. F. (1986): Characterization and isotopic variations in natural waters, *Reviews in Mineralogy*, **16**, 163–183.

Sillitoe, R. H. (2002): Some metallogenic features of gold and copper deposits related to alkaline rocks and consequences for exploration, *Mineralium Deposita*, **37**, 105–117.

Sillitoe, R. H. (2008): Major gold deposits and belts of the North and South American Cordillera: distribution, tectonomagmatic settings and metallogenic consideration, *Economic Geology*, **103**, 663–687.

Song, R., Zhao, Z. (1996): *Geology of the Dongping Gold Deposit Related to an Alkaline Complex in Hebei Province* – Seismological Publishing House, Beijing, 181 p. (in Chinese).

Song, Y., Frey, F. A. (1989): Geochemistry of peridotite xenoliths in basalts from Hannuoba, Eastern China. Implications for sub-continental mantle heterogeneity, *Geochimica et Cosmochimica Acta*, **53**, 97–114.

Sun, J. F., Yang, J. H., Wu, F. Y., Wilde, S. A. (2012): Precambrian crustal evolution of the eastern North China Craton as revealed by U-Pb ages and Hf isotopes of detrital zircons from the Proterozoic Jing'eryu formation, *Precambrian Research*, 200–203, 184–208.

Tian, Z. Y., Han, P., Wu, K. D. (1992): The Mesozoic–Cenozoic East China rift system, *Tectonophysics*, **208**, 341–363.

Tu, G. S., Gao, Z. M., Zhang, Q., Li, Z. Y., Zhao, Z. H., Zhang, B. G. (2004): *Geochemistry and Metallogeny of Dispersed Elements*, Geological Publishing House, Bejing, pp 268–317 (in Chines with English abstract).

Wan, Y. S., Liu, D. Y., Song, B., Wu, J. S., Yang, C., Zhang, Z. Q., Geng, Y. S. (2005): Geochemical and Nd isotopic compositions of 3.8 Ga meta-quartz dioritic and trondhjemitic rocks from the Anshan area and the geological significance, *Journal of Asian Earth Sciences*, **24**, 563–575.

Wang, L. G., Qiu, Y. M., Mcnaughton, N. J., Groves, D. I., Luo, Z. K., Huang, J. Z., Miao, L. C., Liu, Y. K. (1998): Constraints on crustal evolution and gold metallogeny in the northwestern Jiaodong Peninsula, China, from SHRIMP U–Pb zircon studies of granitoids, *Ore Geology Reviews*, **13**, 275–291.

Wang, W., Yang, E., Zhai, M., Wang, S., Santosh, M., Du, L., Xie, H., Lü, B., Wan, Y. (2013): Geochemistry of 2.7 Ga basalts from Taishan area: Constraints on the evolution of early Neoarchean granite-greenstone belt in western Shandong Province, *China Precambrian Research*, **224**, 94–109.

Wang, Y., Jiang, X. M., Wang, Z. K. (1990): Characteristics of lead and sulphur isotope of the gold deposits in Zhangjiakou Xuanhua area, Hebei Province, *Contrib Geology of Mineral Resources Research*, **5**, 2, 66–75 (in Chinese with English abstract).

White, D. E. (1974): Diverse origins of hydrothermal ore fluids, *Econonic Geology*, **69**, 954–973.

Wilde, S. A., Zhao, G. C., Sun, M. (2002): Development of the North China Craton during the late Archaean andits final Amalgamation at 1.8 Ga: some speculations on its position within a global Palaeoproteozoic supercontinent, *Gondwana Research*, **5**, 85–94.

Wu, F. Y., Walker, R J., Ren X., Sun, D. Y., Zhou, X. (2003): Osmium isotopic constraints on the age of lithospheric mantle beneath northeastern China, *Chemical Geology*, **196**, 107–129.

Wu, F. Y., Yang, Y. H., Xie, L. W., Yang, J. H., Xu, P. (2006): Hf isotopic compositions of the standard zircons and baddeleyites used in U-Pb geochronology, *Chemical Geology*, **234**, 105–126.

Wu, F. Y., Zhao, G. C., Wilde, S. A., Sun, D. Y. (2005): Nd isotopic constraints on crustal formation in the North China Craton, *Journal of Asian Earth Sciences*, **24**, 523–545.

Xia, X. P., Sun, M., Zhao, G. C., Wu, F. Y., Xu, P., Zhang, J., Luo, Y. (2006): U-Pb and Hf isotopes study of detrital zircons from the Wulashan khondalites: contraints on the evolution of the Ordos Terrane, Western Block, North China Craton, *Earth and Planetary Sciences Letters*, **241**, 581–593.

Xiao, W. J., Windley, B. F., Hao, J., Zhai, M. G. (2003): Accretion leading to collision and the Permian Solonker

suture, Inner Mongolia, China: Termination of the central Asian orogenic belt, *Tectonics*, **22**, 1069–1088.

Yang, J., Gao, S., Chen, C., Tang, Y., Yuan, H., Gong, H., Xie, S., Wang, J. (2009): Episodic crustal growth of North China as revealed by U-Pb age and Hf isotopes of detrital zircons from modern rivers, *Geochimica et Cosmochimica Acta*, **73**, 2660–2673.

Yang, J. H., Wu, F. Y., Wilde, S. A. (2003): A review of the geodynamic setting of large scale late Mesozoic gold mineralization in the North China Craton: an association with lithospheric thinning, *Ore Geology Reviews, 23*, 125–152.

Yang, J. H., Wu, F. Y., Shao, J. A., Wilde, S. A., Xie, L. W., Liu, X. M. (2006): Constraints on the timing of uplift of the Yanshan fold and thrust belt, North China Craton, *Earth and Planetary Sciences Letters.* **246**, 336–352.

Yin, J. Z., Zhai, Y. S. (1994): On the metallogenic series of gold deposits in Zhangjiakou Xuanhua region, *Hebei J Guilin Coll Geol.* **14**, 359–369 (in Chinese with English abstract).

Yin, J. Z. (1994): S isotopic features of the major gold deposits in the Northwestern Hebei Province, *Gold Science and Technology*, **2** (3), 33–39 (in Chinese).

Zartman, R. E., Smith, J. V. (2009): Mineralogy and U-Th-Pb age of a uranium-bearing jasperoid vein, Sunshine Mine, Coeur d'Alene district, Idaho, USA, *Chemical Geology*, **261**, 185–195.

Zhai, M. G., Santosh, M. (2011): The early Precambrian odyssey of North China Craton: a synoptic overview, *Gondwana Res.* **20**, 6–25.

Zhai, M. G., Santosh, M (2013): Metallogeny of the North China Craton: link with secular changes in the evolving Earth, *Gondwana Res.,* **24**, 275–297.

Zhang, J., Zhao, G. C., Li, S. Z., Sun, M., Liu, S. W. (2012): Structural and aeromagnetic studies of the Wutai Complex: Implications for the tectonic evolution of the Trans-North China, *Orogen Precambrian Research,* 222–223, 212–229.

Zhang, J. H., Jiang, S. H., Nie, F. J. (2005): Geological features of the Hougou and Huangtuliang gold deposits, north-western Hebei Province. In: Jiang, SH, Zhang, JH, Nie, FJ (Eds). *Field Trip Guide No 7, Intrusion-Related Gold Deposits of the Northern Margin of the North China Craton, Hebei Province, China, 8th Biennial SGA Meeting, 18–21 August 2005*, Beijing, China, 12 p. (in Chinese).

Zhang, P. H., Zhao, Z. H., Bao, Z. W., Wang, Y. X., Li, S. Z., Zhang, Y. H. (2001): The distribution pattern of gold and tellurium and their correlation of ores from the Dongping gold mine, *Geology Prospect*, **37**(3), 24–28 (in Chinese with English abstract).

Zhang, P. H., Zhao, Z. H., Zhu, J. C., Zhang, W. L., Bao, Z. W., Zhang, Y. H. (2002): Tellurides of gold and silver and their capacity of carrying gold in ores from the Dongpingtype gold deposits Hebei Province, *China Acta Petrologica Sinica,* **28**(2), 637–651 (in Chinese with English abstract).

Zhang, Z., Mao, J. (1995): Geology and geochemistry of the Dongping gold telluride deposit, Hebei Province, North China, *International Geology Review*, **37**, 1094–1108.

Zhang, Z. C. (1996): Characteristics of H and O isotopes and fluid evolution in Dongping gold deposit, *Gold Geology*, **2**, 36–41 (in Chinese with English abstract).

Zheng, J., Griffin, W. L., O'reilly, S. Y., Liu, J. G., Zhang, R. Y., Lu, F. (2005): Late Mesozoic-Eocene mantle replacement beneath the eastern North China Craton: evidence from Paleozoic and Cenozoic peridotite xenoliths, *International Geology Review*, **47**, 457–472.

Р е з и м е

ГЕНЕЗА НА ЗЛАТО-ТЕЛУРИДНОТО НАОЃАЛИШТЕ ДОНГПИНГ, СЕВЕРНА КИНА, ОСНОВАНА НА ГЕОХЕМИСКИТЕ КАРАКТЕРИСТИКИ НА ФЛУИДИТЕ, ОДРЕДУВАЊЕТО НА СТАРОСТА СПОРЕД СТАБИЛНИТЕ И РАДИОГЕНИ ИЗОТОПИ ^{40}Ar /^{19}Ar,

Mamady Cisse[1*], Xinbiao Lü[2], Munir Mohammed Abdalla Adam[2], Ladislav A. Palinkaš[3], Algeo J. Thomas[4,5]

[1]Институт за минерални суровини и геологија на Боке, Конакри, БП: 84, Република Гвинеја
[2]Факултет за ресурси на Земјата, Кинески универзитет за геолошки науки, Вухан, провинција Хубеи 430074, Кина
[3]Универзитет во Загреб, Природо-математички факултет, Оддел за геологија, Хорватовац 95, 10 000 Загреб, Хрватска
[4]Главна државна лабораторија за биогеологија и геологија на животната средина,
Кинески универзитет за геолошки науки, Вухан, провинција Хубеи 430074, Кина
[5]Универзитет во Синсинати, Оддел за геологија, Синсинати, OX 45221-0013, С.А.Д.
mcisseismgb@yahoo.fr

Клучни зборови: област Чонгли; наоѓалиште Донгпинг; одредување старост според ^{40}Ar/^{39}Ar; стабилни и радиогени изотопи; рудоносни флуиди; наоѓалиште на злато; Северна Кина

Златоносното поле Донгпинг се наоѓа во алкалниот комплекс Шуикуангоу на западните Јаншан Планини во провинцијата Хебеи, на северната маргина од Севернокинескиот Кратон. Тоа е едно од најголемите златоносни наоѓалишта во Кина, со планирано производство на злато од 2.57 тони годишно за времетраење од 12 години.

Наоѓалиштето на злато Донгпинг е богато со елементите Au, Te, Ag, Pb, Bi, Sb и As. Најголем дел од златото е присутно во телуридните минерали калаверит (43% Au, 38% Ag) и пецит (23% Au, 46% Ag). Минерализацијата на злато главно е во K-фелдспатнокварцните штокверци, жици и расеани сулфиди. Наоѓалиштето содржи три вида

руда кои се разликуваат по нивните минерални асоцијации: жично-кварцно злато, злато во телуриди и расеано злато. Парагенезата на рудата покажува три различни хидротермални фази, од кои втората е најбогата на рудата. Староста на рудата, утврдена според $^{40}Ar/^{39}Ar$ во примероците на К-фелдспат, укажува на две епизоди на златоносна минерализација, на 154,89 ± 0,70 Ma и 176,93 ± 4,66 Ma. Староста на златоносната минерализација укажува дека таа следела по интрузијата на девонските гранити, но делумно се поклопува со можната магматска активност во јура и креда. Температурата на хомогенизацијата на повеќето гасно-течни инклузии се движи од 120 до 240 °C и од 240 до 400 °C. Гаснотечните инклузии во кварцните жици се богати со CO_2 и се карактеризираат со низок салинитет (просечно 6,0–8,8 теж.% NaCl eq.). Раманските спектри одредени со ласер во гасно-течните инклузии покажуваат дека течните фази се богати главно со вода, но исто така содржат и CO_2.

Водородноизотопниот состав на (δ^2H) во гасно-течните инклузии се движи од –100,3 до –66,5 ‰, а пресметаниот изотопен состав на кислородот ($\delta^{18}O$) за изворните флуиди се движи од –0,3 до +6,9 ‰ "стандардна просечна океанска вода" (SMOW). Овие вредности покажуваат дека рудоносниот флуид доаѓа од длабок магматски хидротермален систем, со вклучување на метеорска вода и можеби и вода под влијание на органска материја. Сулфурните изотопни состави ($\delta^{34}S$) на пиритот главно се од –0,3 до –13,6 ‰ според стандардот Vienna Cañon Diablo Troilite (VCDT), што укажува на хомогеност на сулфур во магматскиот извор со последователно фракционирање при релативно оксидирачки услови во рудоносните кварцни жици. Односот на $\delta^2H_{H_2O}$ и $^{87}Sr/^{86}Sr$ укажува на тоа дека гасно-течните инклузии и околните гранитоидни карпи биле под влијание на мешани магматски и метеорски води.